MC3T3-E1 osteoblast attachment and proliferation on porous hydroxyapatite scaffolds fabricated with nanophase powder

Ian O Smith[1]
Laura R McCabe[2]
Melissa J Baumann[1]

[1]Department of Chemical Engineering and Materials Science, [2]Department of Physiology, Michigan State University, East Lansing, MI, USA

Abstract: Porous bone tissue engineering scaffolds were fabricated using both nano hydroxyapatite (nano HA) powder (20 nm average particle size) and micro HA powder (10 μm average particle size), resulting in sintered scaffolds of 59 vol% porosity and 8.6±1.9 μm average grain size and 72 vol% porosity and 588±55 nm average grain size, respectively. Scanning electron microscopy was used to measure both the grain size and pore size. MC3T3-E1 osteoblast (OB) attachment and proliferation on both nano HA and micro HA porous scaffolds were quantified. As expected, OB cell number was greater on nano HA scaffolds compared with similarly processed micro HA scaffolds 5 days after seeding, while OB attachment did not appear greater on the nano HA scaffolds ($p<0.05$).

Keywords: hydroxyapatite, osteoblast, nanomaterial, porous, scaffold

Introduction

Bone is a composite material having a calcium phosphate (CaP) mineral component and a collagen-based organic matrix. CaP is a bioceramic resembling hydroxyapatite (HA, $Ca_{10}(PO_4)_6(OH)_2$), where the individual crystals have a plate-like morphology, 15–200 nm in length and 10–80 nm in width with a thickness between 2 and 7 nm (Fratzl et al 2004). These apatite crystals are embedded within the collagen fiber component of the organic matrix, which forms lamellar sheets comprising the concentric rings of osteons in cortical bone (Young and Heath 2000) and the more woven structure of trabeculae in cancellous bone (Hassenkam et al 2004). The collagen matrix is composed primarily of Type I collagen fibers of approximately 100 nm in diameter (Fratzl et al 2004).

These nano-components play an active role in bone development and growth. Collagen fibers act as the scaffold on which newly formed nanocrystals of bone apatite form and grow, leading eventually to the formation of woven bone. This primitive early phase of bone is eventually replaced by the lamellae of adult bone (Young and Heath 2000). Additionally, collagen fibers have been shown to incorporate into porous HA tissue engineering scaffolds where the interfacial zone between bone and scaffold has been found to be a nano HA-reinforced collagen matrix (Chen et al 2004).

One area of current research in biomimetic nano-scale ceramic bone substitute materials is therefore focused on the design of nanoscale ceramic–polymer composites to mimic some of the morphological features of natural bone. These systems can be grouped into three categories: nano-CaP–collagen (Du et al 1998; Du et al 1999; Sakane et al 2004), nano-CaP–noncollagen polymer (Wei et al 2003, 2004a, 2004b), and a combination of the two (Cui et al 2004; Liao et al 2004). Although there are several types of CaP bioceramics, HA is the most commonly used, having a chemistry that closely matches that of normal bone apatite (Jarcho 1981; Hench 1998; Li et al 2004).

Correspondence: Melissa J Baumann
CHEMS Dept 2527 Engineering Bldg, Michigan State University, East Lansing, MI 48824-1226, USA
Tel +1 517 355 5135
Fax +1 517 432 1103
Email mbaumann@msu.edu

Nanocrystalline HA has been shown to be biocompatible with a minimal inflammatory response (Huang et al 2004; Silva et al 2004), although there is a potential for cytotoxicity (Huang et al 2004). While some engineered nano-CaP–polymer composites such as HA–collagen polylactic acid (PLA) scaffolds have been reported to show improvements in compressive strength using nano HA (Liao et al 2004), they did not replicate the hierarchical structure of bone which may be crucial in encouraging bone ingrowth into a tissue engineered scaffold (Du et al 1998; Liao et al 2004). Also, Yoneda et al (2004) confirm that the degradation of PLA adversely affects cell behavior, specifically that increased degradation leads to a decrease in cell spreading, adhesion, and cell survival. Therefore, current research focuses on developing a bioceramic with a morphological structure similar to that of normal bone to promote bone regeneration in vitro and in vivo (Longsworth and Eppell 2002).

Webster et al compared changes in osteoblast (OB) behavior on nano-grained versus micro-grained dense bioceramics, including Al_2O_3, TiO_2, and HA, demonstrating increases in OB attachment (Webster, Ergun, et al 1999; Webster et al 1999a, 1999b) and proliferation, alkaline phosphatase (AP) activity, and calcium deposition, as well as decreased cell motility (Webster, Ergun, et al 1999; Webster et al 2000a).

Osteoblast attachment on a bioinert ceramic like Al_2O_3 can be attributed to the presence of physical surface irregularities that lead to increased morphological fixation (Hench 1998). Such fixation in turn plays an important role in the use of TiO_2 as a coating for orthopedic implants, improving the integrity of the implant–bone interface (Areva et al 2004). Fixation also plays a role in OB attachment to HA, but increased osteoblast adhesion may also occur because of improved protein interactions that have been linked to decreases in grain size (Webster et al 2000b).

Enhanced OB behavior for HA having a finer grain size is further illustrated in a study by Xie et al (2004), which recently reported that MC3T3-E1 OBs seeded onto dense HA discs showed differences in gene expression related to grain boundary surface area. Gene expression of OBs on HA discs fabricated with an average particle size of 35 μm suggest a decrease in cellular metabolism and an increase in differentiation while HA discs processed from smaller particle sizes (~11 μm) showed gene expression profiles consistent with increased cell growth. Each of the previous studies was conducted using dense ceramic scaffolds, designed specifically for cell culture purposes, while the current study assesses whether porous bone replacement scaffolds fabricated with nano HA powder rather than micro HA improves OB attachment and proliferation.

Materials and methods

HA powder, of 10 μm average particle size, was purchased from Hitemco Medical (Old Bethpage, NY, USA) and used in its as-received form. Nano-scale HA powder having an average particle size of 20 nm was purchased from Berkeley Advanced Biomaterials (San Leandro, CA, USA). The nano HA powder arrived in an ammonium hydroxide suspension which was subsequently centrifuged, resuspended in ethanol, centrifuged again to separate out the nano HA powder, and then vacuum dried for 12 hours before use (per manufacturer instructions).

Methods used in this study can be divided into four parts: scaffold fabrication, imaging of scaffold surfaces, osteoblast cell culture, and assessment of OB attachment and proliferation.

Porous cylindrical samples of each HA powder particle size were foamed by suspending the HA powders in KNO_3 electrolyte to which H_2O_2 had been added, pouring the resulting foamed suspension into cylindrical molds and drying at 125°C. The dry, green HA samples were then sintered at 1100°C for 1 hour (nano HA) following the procedure established by Webster et al (Webster, Ergun, et al 1999; Webster et al 2000a, 2000b) or 1360°C for 4 hours (micro HA) using a protocol developed by McMullen (2004). Both the micro and nano HA-sintered scaffolds were next sectioned using a Buehler IsoMet 1000 diamond abrasive wafering saw (Buehler, Lake Bluff, IL, USA) into discs of approximately 1mm thickness and autoclaved.

Nano HA and micro HA scaffold surfaces were observed using scanning electron microscopy (SEM). Samples were coated with a thin layer of Au, approximately 21 nm thick, using an Emscope SC500 sputter coater (Emscope Laboratories Ltd, Ashford, UK), mounted onto Al stubs and imaged using a JEOL 6400 SEM (JEOL Corporation, Tokyo, Japan) operated at an accelerating voltage of 5keV. SEM photomicrographs were collected and exported using the AnalySIS software package.

MC3T3-E1 OBs of passage 22–23, cultured in alpha minimum essential medium (α-MEM) supplemented with 10% fetal bovine serum (FBS), were trypsinized, resuspended in α-MEM, and seeded evenly across the surface of porous HA scaffolds at a density of 11320 cells/cm^2 and incubated in air at 37°C, 5% CO_2, and high humidity (Shu et al 2003). 2 mL of α-MEM was added per specimen and was replenished every 2 days. Three specimens were statically cultured per time interval and 2 sets of cultures were examined, resulting

in 6 samples per time interval. MC3T3-E1 OBs are a widely used OB cell line (Cerroni et al 2002; Werner et al 2002; Shu et al 2003; Iyer et al 2004; Xie et al 2004) that have been shown to behave in a similar manner to primary OBs (Griffin et al 2005).

OB attachment was assessed at intervals of 0.5, 1, 2, and 4 hours. Scaffolds were removed, placed into separate wells, rinsed with phosphate-buffered saline (PBS), trypsin/α-MEM (50/50) added, and the scaffolds morselized to facilitate osteoblast detachment. Media was drawn from each well and the OBs counted using a hemacytometer. OB cell counts were also conducted at 1, 3, and 5 days following attachment to assess OB proliferation.

Statistical differences between attachment and growth on micro HA and nano HA scaffolds were calculated using Student's t tests. A p value of 0.05 or lower was considered to be significant.

Results

Porous HA scaffolds were successfully fabricated by foaming and sintering both micro HA and nano HA powder as described in the previous section. SEM showed that the micro HA scaffolds have a grain size of 8.6±1.9 μm which is approximately 15 times greater than the nano HA grain size of 588±55 nm (representative micrographs given in Figure 1). The average grain size was determined using a line-intercept method (n=50) based on ASTM standard E 112 (ASTM 2004). The volume porosity of micro HA and nano HA scaffolds using Archimedes method were found to be 59 vol% and 72 vol %, respectively (McMullen 2004). Both micro and nano HA scaffold surfaces consisted of grains which are the sintered particles interspersed with frequent gaps along with larger macropores–micropores of 390±210 μm–38±22 μm for micro HA and 480±275 μm–30±21 μm for nano HA. These size ranges fall within standard macropore (200 μm–400 μm) and micropore (<60 μm) ranges reported by deGroot et al (1988). A representative SEM photomicrograph showing the nature and distribution of the porosity within the pore wall of a nano HA scaffold is given in Figure 2.

Contrary to published data by Webster et al using dense HA scaffolds, these results show that initial OB attachment does not increase as a function of decreased grain size on porous HA scaffolds (Webster, Ergun, et al 1999; Webster et al 2000a, 2000b, 2001). MC3T3-E1 OB attachment on porous scaffolds is plotted as a function of time for 0.5, 1, 2, and 4 hours (Figure 3). Based on hemacytometer analysis, OB attachment on the micro HA scaffolds appears greater than on the nano HA scaffolds and differences were statistically significant (with $p<0.05$).

When OB cell number is examined, the mean values for OB proliferation on nano HA scaffolds are higher compared with the mean values on micro HA scaffolds (Figure 4) at 1, 3, and 5 days' culture time. Differences in proliferation between micro HA and nano HA scaffolds at 1 and 3 days were not found to be statistically significant, with $p>0.05$ in both cases ($p=0.64$ and $p=0.12$, respectively). However, at 5 days, differences in osteoblast number were found to be significant ($p<0.05$).

Discussion

Porous bioceramic scaffolds offer advantages over dense substrates for bone tissue engineering applications, because

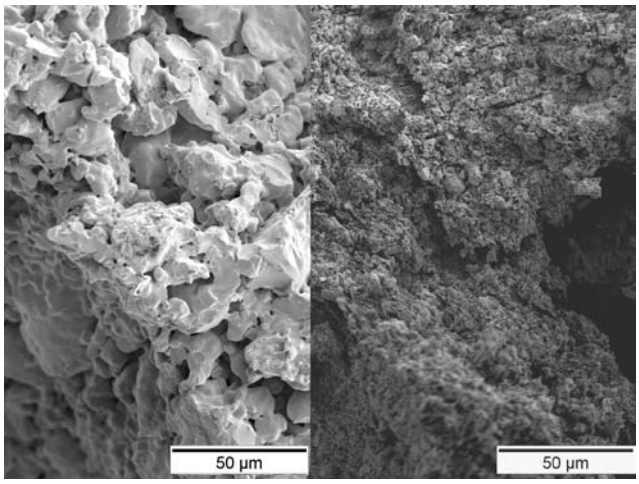

Figure 1 Comparison of SEM micrographs of the surface of scaffolds fabricated using micro HA (left) and nano HA (right).
Abbreviations Figures 1–4: HA, hydroxyapatite, OB, osteoblast.

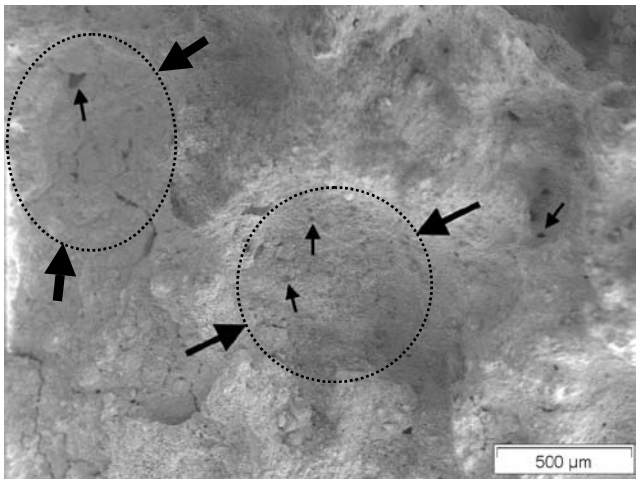

Figure 2 SEM micrograph showing the surface of porous scaffold fabricated using nano HA, including macropores (large arrows noting approximate boundary of a macropore) and micropores (small arrows emphasizing the <60 μm interconnecting pores).

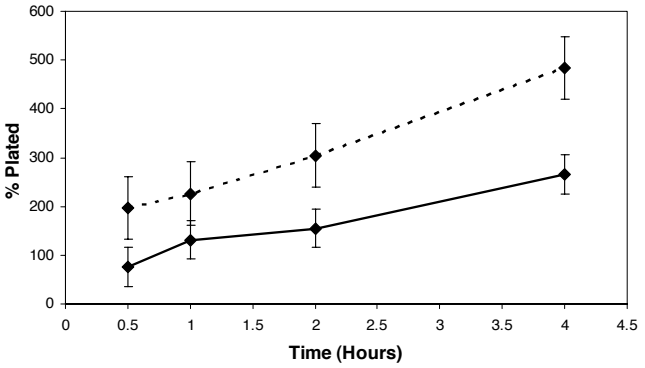

Figure 3 MC3T3-E1 OB attachment on micro HA (dashed line) and nano HA (solid line) scaffolds as a function of time, at intervals of 0.5, 1, 2, and 4 hours. Values are mean±SE, $p<0.05$ at all time intervals for comparison of nano HA with micro HA.

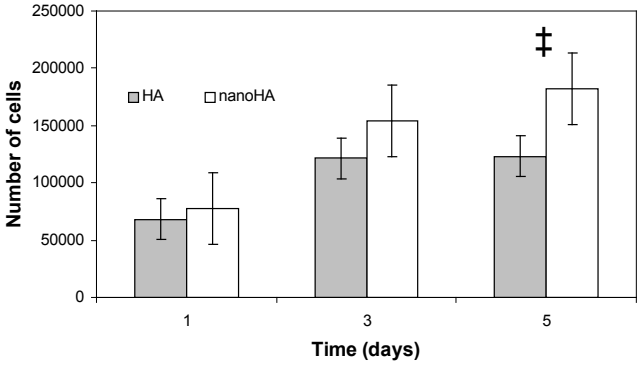

Figure 4 MC3T3-E1 OB proliferation on micro HA and nano HA, after periods of 1, 3, and 5 days. Values are mean±SE, $p>0.05$ for comparison of nano HA with micro HA porous scaffold for 1 and 3 days. $p<0.05$ for 5 days (‡).

they present a more complex interface for bone ingrowth that more closely mimics natural bone (Hench 1998; Hulbert et al 1970, 1972). Additionally, porous CaP ceramics are capable of promoting osteoprogenitor attachment and new bone formation (Ohgushi et al 1990). Osteoprogenitor cells cultured on porous HA have been shown to produce extracellular matrix in vivo, a precursor to bone formation (Ohgushi et al 1990). Therefore, it is important to observe the effect of HA grain size reduction on OB behavior and to examine these differences for porous scaffolds which are more suited for bone tissue engineering applications.

Foaming and sintering nano HA with a particle size of 20 nm yielded porous scaffolds of submicron grain size (588 nm±55 nm). While this grain size is not truly nanoscale (<100 nm), it is small enough to assess the effect of grain size reduction (15x) on OB behavior in vitro. This reduction in grain size means that there is an increased grain boundary surface area, which has been tied to increased OB attachment (Perla et al 2004) and enhanced gene expression (Xie et al 2004) indicative of increased cell growth and differentiation. Reduction in grain size has also been linked to increased surface roughness, which in turn has been shown to increase OB adhesion, proliferation, AP activity, and calcium production (Webster 2001). In future studies, atomic force microscopy (AFM) will be used to measure the surface roughness of these scaffolds, to determine whether these results are repeatable for porous HA.

Webster et al have repeatedly shown that a large decrease in HA grain size produces changes in osteoblast activity, including improvements in attachment and proliferation (Webster, Ergun, et al 1999; Webster et al 2000a, 2000b, 2001). Results of this study both contradict (OB attachment) and reinforce (OB proliferation) these findings. Our study shows that OB attachment did not improve on scaffolds fabricated from nano HA powder compared with those produced from micro HA powder. However, each of Webster's studies used dense HA having a sintered grain size of 67 nm (Webster et al 2000a, 2000b), which is ~11% of our sintered grain size and only 1/3 larger than their unsintered particle size. In contrast, our scaffolds have grains 30 times larger than our unsintered particles. This difference in grain growth in our scaffolds, from 20 nm–588±55 nm, is likely an artifact of the highly porous nature of our scaffolds in which the predominant sintering mechanism is coarsening (Barsoum 1997). Future studies will investigate the sintering behavior of these foamed nano HA scaffolds with the goal of reducing grain growth to yield true high volume porosity nanograined HA scaffolds.

At each time period, 0.5, 1, 2, and 4 hours, hemacytometer analyses suggest an increase in cell number (attachment) on micro HA scaffolds compared with nano HA scaffolds. This suggests that increased grain size is not positively related to OB attachment behavior in highly porous scaffolds. However, the cell attachment values for both scaffolds are much larger in this study than expected. This suggests that HA particles themselves may have been included in the cell counting analyses. This was a more significant issue when counting the OBs from the micro HA scaffolds where the morselized scaffold particles were of a similar size in comparison with the OBs. In contrast, the nano HA scaffolds morselized into significantly smaller fragments that were easily distinguishable from the much larger OBs. This is reflected in the apparent and uniform shifting upwards of the OB attachment data in Figure 3 for the micro HA. However, as this experimental cell counting technique was consistently applied, the differences noted at day 5 in Figure 4 are still significant. Future studies will be done by normalizing such attachment and proliferation data against a background count of morselized scaffold without cells.

While OB attachment did not increase with decreased grain size, the mean OB proliferation, measured at 1, 3, and 5

days, on nano HA scaffolds was higher than the mean values for the micro HA scaffolds. This indicates that proliferation may be driven by increased grain boundary area resulting from the smaller grain size, in addition to the optimum morphology in terms of pore size and pore interconnectivity (eg macro and microporosity) presented by our highly porous scaffolds. The basis for OB–HA adhesion and the effect of grain boundary volume on OB behavior are not completely understood, but may be linked in part to protein interactions at the surface (Webster et al 2000b). Webster et al (2000b) found that a decrease in grain size promoted an increase in vitronectin and collagen concentration and a decrease in albumin, laminin, and fibronectin concentration. They also linked the protein stereochemical structure to grain size and surface topography of bioceramic substrates (Webster et al 2000b). Based on these findings, FBS proteins may adsorb more readily to nano HA scaffolds compared with micro HA scaffolds in this study, but this was not verified. The effect of FBS protein adsorption in vitro, contrasted with protein adsorption in an in vivo environment, should be investigated.

Other approaches to increasing OB attachment and proliferation on HA surfaces include peptide coating. For example, EEEEEEEPRGDT coating increased attachment at 30 minutes compared with an HA control (Itoh et al 2002). GRGDSPC and cyclo-DfKRG increase osteoprogenitor cell attachment at 3 and 24 hours compared with untreated hydroxyapatite (Durrieu et al 2004). While these coatings increased OB attachment and proliferation, the smaller grain size found in our HA scaffolds is an intrinsic property, reducing the need for post-fabrication scaffold treatments such at the peptide coatings of Itoh et al (2002) and Durrieu et al (2004).

Although the use of nano HA in porous bone scaffolds does not initially improve OB attachment by 4 hours' culture time, the apparent increase in proliferation of OBs at day 5 shows the potential for more rapid osteoblast growth, and presumably more rapid calcification and bone formation in vitro. While further studies must be conducted to measure OB differentiation and calcium production over time in vitro, nano HA porous bone scaffolds, because of their increased grain boundary area and optimum pore size and interconnectivity, show promise as an effective bone scaffold for use in bone tissue engineering applications.

Acknowledgements

The authors acknowledge the use of the SEM facilities at the Advanced Microscopy Center, Michigan State University along with the assistance of Mr J Quast with the SEM imaging.

References

Areva S, Paldan H, Peltola T, et al. 2004. Use of sol-gel-derived titania coating for direct soft tissue attachment. *J Biomed Mater Res*, 70A:169–78.

ASTM. 2004. E112-96 Standard test methods for determining average grain size. ASTM International.

Barsoum M. 1997. Fundamentals of ceramics. New York: McGraw-Hill.

Cerroni L, Filocamo R, Fabbri M, et al. 2002. Growth of osteoblast-like cells on porous hydroxyapatite ceramics: an in vitro study. *Biomol Eng*, 19:119–24.

Chen QZ, Lu WW, Wong CT, et al. 2004. Role of collagen fibres in bone-bonding of crystalline hydroxyapatite implant. 7th World Biomaterials Congress. 2004 May 17–24, 2004; Sydney, Australia. p 1439.

Cui FZ, Zhang W, Liao, SS. 2004. Hierarchical self-assembling of nano-fabril of mineralized collagen for bone graft. 7th World Biomaterials Congress. 2004 May 17–24, 2004; Sydney, Australia. p 1004.

deGroot K. 1988. Effect of porosity and physicochemical properties on the stability, resorption, and strength of calcium phosphate ceramics. *Ann N Y Acad Sci*, 523:227–33.

Du C, Cui FZ, Feng QL, et al. 1998. Tissue response to nano-hydroxyapatite/collagen composite implants in marrow cavity. *J Biomed Mater Res*, 42:540–8.

Du C, Cui FZ, Zhu XD, et al. 1999. Three-dimensional nano HAp/collagen matrix loading with osteogenic cells in organ culture. *J Biomed Mater Res*, 44:407–15.

Durrieu MC, Pallu S, Guillemot F, et al. 2004. Grafting RGD containing peptides onto hydroxyapatite to promote osteoblastic cells adhesion. *J Mater Sci Mater Med*, 15:779–86.

Fratzl P, Gupta HS, Paschalis EP, et al. 2004. Structure and mechanical quality of the collage-mineral nano-composite in bone. *J Mater Chem*, 14:2115–23.

Griffin MA, Smith IO, Baumann MJ. 2005. Comparison between primary and clonal osteoblast cells for in vitro attachment studies to hydroxyapatite. Ceramic Transactions, v 164, Bioceramics: Materials and Applications V – Proceedings of the 106th Annual Meeting of the American Ceramic Society. 2004 April 18–21. p 83–9 .

Hassenkam T, Fantner GE, Cutroni JA, et al. 2004. High-resolution AFM imaging of intact and fractured trabecular bone. *Bone*, 35:4–10.

Hench LL. 1998. Bioceramics. *J Am Ceram Soc*, 81:1705–28.

Huang J, Best SM, Bonfield W, et al. 2004. *In vitro* assessment of the biological response to nano-sized hydroxyapatite. *J Mater Sci Mater M*, 15:441–5.

Hulbert SF, Morrison SJ, Klawitter, JJ. 1972. Tissue response to three ceramics of porous and non-porous structures. *J Biomed Mater Res*, 6:347–74.

Hulbert SF, Young FA, Mathews RS, et al. 1970. Potential of ceramic materials as permanently implantable skeletal protheses. *J Biomed Mater Res*, 4:433–56.

Itoh D, Yoneda S, Kuroda S, et al. 2002. Enhancement of osteogenesis on hydroxyapatite surface coated with synthetic peptide (EEEEEEEPRGDT) *in vitro*. *J Biomed Mater Res*, 62:292–8.

Iyer VV, Kadakia TB, McCabe LR, et al. 2004. CCAAT/enhancer-binding protein-beta has a role in osteoblast proliferation and differentiation. *Exp Cell Res*, 295:128–37.

Jarcho M. 1981. Calcium phosphate ceramics as hard tissue prosthetics. *Clin Orthop Relat Res*, 157:259–78.

Li Z, Yubao L, Wang X, et al. 2004. Comparison of compositions and structural characterizations of synthetic nano-hydroxyapatite and mineral phase from porcine femoral bone. *High Technology Letters*, 10:48–51.

Liao SS, Cui FZ, Zhang W, et al. 2004. Hierarchically biomimetic bone scaffold materials: Nano-HA/collagen/PLA composite. *J Biomed Mater Res*, 69B:158–65.

Longsworth J, Eppell, SJ. 2002. Design and assembly of a sterile nanoscale orthopedic biomaterial. Biomaterials, Proceedings of the Northeast Conference. 2002. p 173–4.

McMullen R. 2004. An *in vitro* investigation of MC3T3-E1 osteoblast proliferation and differentation on hydroxyapatite based tissue-engineered scaffolds. Masters thesis, Department of Chemical Engineering and Materials Science, Michigan State University. p 43–6..

Ohgushi H, Okumura M, Tamai S, et al. 1990. Marrow cell induced osteogenesis in porous hydroxyapatite and tricalcium phosphate: a comparative histomorphometric study of ectopic bone foremation. *J Biomed Mater Res*, 24:1563–70.

Perla V, Ejiofor JU, Webster TJ. 2004. Directed osteoblast adhesion at particle boundaries: Promises for nanophase metals. Symposium on Biological and Bioinspired Materials and Devices. *Mat Res Soc Proc,* 823:207–12.

Sakane M, Mutsuzaki H, Miyanaga Y, et al. 2004. Nano-composites of calcium phosphate-collagen promote osteoclast growth at the interface between tendons and bone tunnels in knee ligament reconstruction. 7th World Biomaterials Congress. 2004 May 17–24, 2004; Sydney, Australia.p 385.

Shu R, McMullen R, Baumann MJ, et al. 2003. Hydroxyapatite accelerates differentiation and suppresses growth of MC3T3-E1 osteoblasts. *J Biomed Mater Res*, 67A:1196–204.

Silva CC, Pinheiro AG, de Oliveira RS, et al. 2004. Properties and *in vivo* investigation of nanocrystalline hydroxyapatite obtained by mechanical alloying. *Mat Sci and Eng C*, 24:549–54.

Webster TJ, Ergun C, Doremus RH, et al. 1999. Nanocrystalline hydroxyapatite enhances osteoblast function. First Joint BMES/EMBS Conference. 1999 October 13–16; Atlanta, GA. p 744.

Webster TJ, Ergun C, Doremus RH, et al. 2000a. Enhanced functions of osteoblasts on nanophase ceramics. *Biomaterials*, 21:1803–10.

Webster TJ, Ergun C, Doremus RH, et al. 2000b. Specific proteins mediate enhanced osteoblast adhesion on nanophase ceramics. *J Biomed Mater Res*, 51:475–83.

Webster TJ, Siegel RW, Bizios R. 1999a. Design and evaluation of nanophase alumina for orthopaedic/dental applications. *Nanostruct Mater*, 12:983–6.

Webster TJ, Siegel RW, Bizios R. 1999b. Osteoblast adhesion on nanophase ceramics. *Biomaterials*, 20:1221–7.

Webster TJ, Siegel RW, Bizios R. 2001. Nanoceramic surface roughness enhances osteoblast and osteoclast functions for improved orthopaedic/dental implant efficacy. *Scripta Mater*, 44:1639–42.

Wei J, Li Y, Chen W, et al. 2003. A study on nano-composite of hydroxyapatite and polyamide. *J Mater Sci*, 38:3303–6.

Wei J, Yubao L, Xuelig P, et al. 2004a. Injectable apatite and ploymer biomimetic nano-composite cement for bone tissue engineering. 7th World Biomaterials Congress. 2004 May 17–24, 2004; Sydney, Australia. p 1359.

Wei J, Yubao L, Xuelig P, et al. 2004b. A study on tissue engineering scaffold material of nano-apatite and polyamide composite. 7th World Biomaterials Congress. 2004 May 17–24, 2004; Sydney, Australia. p 827.

Werner J, Linner-Krcmar B, Friess W, et al. 2002. Mechanical properties and in vitro cell compatibility of hydroxyapatite ceramics with graded pore structure. *Biomaterials*, 23:4285–94.

Xie J, Baumann MJ, McCabe LR. 2004. Osteoblasts respond to hydroxyapatite surfaces with immediate changes in gene expression. *J Biomed Mater Res*, 71A:108–17.

Yoneda S, Guthrie WF, Bright DS, et al. 2004. In vitro biocompatibility of hydrolytically degraded poly(d,l-lactic acid). 7th World Biomaterials Congress. 2004 May 17–24, 2004; Sydney, Australia.p 1324.

Young B, Heath JW. 2000. Wheater's functional histology. Edinburgh: Churchill Livingstone.